



# EGF receptor is involved in WNT3a-mediated proliferation and motility of NIH3T3 cells via ERK pathway activation

Sung-Eun Kim, Kang-Yell Choi \*

National Research Laboratory of Molecular Complex Control, Department of Biotechnology, Yonsei University, Seoul 120–749, South Korea

Received 20 December 2006; received in revised form 6 February 2007; accepted 6 February 2007

## Abstract

WNT3a stimulates proliferation of NIH3T3 cells via activation of the extracellular signal-regulated kinase (ERK) pathway. The RAF-1→MEK→ERK cascade was immediately increased by WNT3a treatment, however, the upstream event triggering ERK pathway activation by WNT3a is not clear. WNT3a activated RAS and WNT3a-induced ERK activation was blocked by dominant-negative RAS, indicating that WNT3a might act upstream of RAS. WNT3a-induced ERK pathway activations were blocked by AG1478, the epidermal growth factor receptor (EGFR) inhibitor, and EGFR siRNA. The WNT3a-induced ERK pathway activation was not observed in fibroblasts retaining defective EGFR, but the WNT3a effect was restored by EGFR reconstitution. These results indicate involvement of EGFR in the WNT3a-induced ERK pathway activation. WNT3a-induced motility and cytoskeletal rearrangement as well as proliferation of NIH3T3 cells were blocked by AG1478 and EGFR siRNA or abolished in EGFR knock-out fibroblasts, indicating involvement of EGFR in those cellular processes. WNT3a-induced ERK pathway activation was not affected by Dickkopf-1 (DKK-1), although WNT3a-induced activations of the WNT/β-catenin pathway and proliferation were reduced by DKK-1. EGFR is involved in WNT3a-induced proliferation via both routes dependent on and independent of the WNT/β-catenin pathway. These results indicate that WNT3a stimulates proliferation and motility of NIH3T3 fibroblasts via EGFR-mediated ERK pathway activation.

© 2007 Elsevier Inc. All rights reserved.

**Keywords:** Epidermal growth factor receptor; WNT; cell motility; Cell proliferation; ERK pathway

## 1. Introduction

WNTs are secreted lipid-modified glycoproteins that are involved in the differentiation, proliferation, polarity, motility, and death of cells [1–4]. In the absence of WNT, β-catenin forms a multi-protein complex with adenomatous polyposis coli (APC), Axin, and glycogen synthase kinase 3β (GSK3-β), leading to the proteasomal degradation of β-catenin [5–8]. When WNTs bind to Frizzled receptor [9,10] and LRP 5/6 [11], Disheveled (DSH) is activated and leading to dissociation of the destruction complex followed by cytoplasmic accumulation of β-catenin. The β-catenin translocates into the nucleus and forms a heterodimer with the TCF/LEF transcription factor for activation of target

genes, such as *c-myc* and *cyclin D1* involving transformation [12,13]. The ERK pathway is known to be a major transforming signaling pathway [14–16] activated by stimulation of the receptor tyrosine kinases (RTK) such as epidermal growth factor receptor (EGFR) [17,18]. EGFR is involved in ERK pathway activation by growth factors such as EGF, and RAS is an important mediator of the activation of the ERK pathway.

Recently, we identified the activation of the RAF-1→MEK→ERK cascade by WNT3a, one of the WNTs, in NIH3T3 mouse fibroblasts, and related it to cellular proliferation [19]. However, the upstream event involving ERK pathway activation by WNT3a was not identified. Recent studies also indicated the possibility of the involvement of RTK in WNT-induced activation of the ERK pathway without characterization of the related physiologies [20–22]. WNTs affect the motility of various types of cells [23–26], and the ERK pathway is known to affect EGF-induced cell motility [27,28]. However, no

\* Corresponding author. Tel.: +82 2 2123 2887; fax: +82 2 362 7265.

E-mail address: [kychoi@yonsei.ac.kr](mailto:kychoi@yonsei.ac.kr) (K.-Y. Choi).

evidence is also available for any role of EGFR and ERK pathways in the WNT3a-induced cell motility.

In this study, we investigated the possibility of involvement of EGFR in WNT3a-induced ERK pathway activation, proliferation, and cell motility. The role of EGFR in WNT3a-induced ERK pathway activation and proliferation was tested by measuring the effects of an EGFR specific inhibitor and EGFR small-interference RNA (siRNA) as well as by using cell lines retaining defective EGFR. We also investigated the involvement of RAS in ERK pathway activation by using dominant-negative forms of RAS (dn-Ras). The roles of WNT/ $\beta$ -catenin pathway in WNT3a-induced ERK pathway activation and proliferation were investigated by measuring the effects of Dickkopf-1 (DKK-1), the negative regulator of the WNT signaling function, in interaction with LRP 5/6 [29,30]. The role of EGFR in WNT3a-induced cell migration, invasion, and cytoskeletal rearrangement was also investigated by using the EGFR inhibitor and EGFR siRNA. WNT3a stimulates proliferation and migration of fibroblasts via EGFR-mediated ERK pathway activation. The WNT3a-induced ERK activation was not affected by DKK-1 although activations of the WNT/ $\beta$ -catenin pathway and proliferation were reduced by DKK-1. These results indicate that WNT3a-induced immediate ERK activation occurs regardless of WNT/ $\beta$ -catenin signaling. However, proliferation by WNT3a involving EGFR is attributed to both WNT/ $\beta$ -catenin involving Tcf/ $\beta$ -catenin mediated transcription and immediate signaling activation of ERK pathway. The proliferation by WNT3a is highly complex, and could occur by complex signaling cross-talk involving EGFR as indicated by down-regulation of  $\beta$ -catenin level by EGFR $-/-$  fibroblasts and EGFR siRNA. Overall, we identified the role of EGFR in WNT3a-induced ERK pathway activation involving proliferation, motility and cytoskeletal rearrangement. WNT/ $\beta$ -catenin and the ERK pathway interact at various levels in the regulation of cellular physiologies related to cell growth.

## 2. Materials and methods

### 2.1. Reagents

Dulbecco's Modified Eagles Medium (DMEM), RPMI1640, fetal bovine serum (FBS), penicillin–streptomycin, and Lipofectamine plus reagent were purchased from Life Technologies (Grand Island, NY). The antibodies for ERK, phospho-ERK (p-ERK) and  $\beta$ -catenin were purchased from Santa Cruz Biotechnology (Santa Cruz, CA). phospho-MEK (p-MEK) and horseradish peroxidase (HRP)-conjugated secondary anti-mouse IgG antibodies were acquired from Cell Signaling Biotechnology (Beverly, MA). HRP-conjugated goat anti-rabbit IgG antibody was obtained from Bio-Rad laboratories (Hercules, CA). The phospho-RAF-1/Ser-338 (p-RAF-1) and Pan-RAS antibodies were purchased from Upstate Biotechnology (Lake Placid, NY). The  $\alpha$ -tubulin and H-RAS antibodies were obtained from Oncogene Research Products (San Diego, CA). Recombinant mouse WNT3a and recombinant mouse DKK-1 were purchased from R&D Systems Product (Minneapolis, MN). An enhanced chemiluminescence (ECL) system was acquired from Amersham Pharmacia (Uppsala, Sweden). A *Silencer*<sup>TM</sup> siRNA construction kit was acquired from Ambion (Austin, TX). AG1478 was purchased from Calbiochem (La Jolla, CA), and a protein assay solution was obtained from Bio-Rad Laboratories. 4', 6'-diamidine-2'-phenylindole dihydrochloride

(DAPI) was bought from Boehringer Mannheim (Mannheim, Germany), Alexa Fluor 488 goat anti-mouse IgG and Alexa Fluor 488 phalloidin were purchased from Molecular Probe (Eugene, OR), and anti-BrdU monoclonal antibody was acquired from DAKO (Carpinteria, CA). All of the other chemicals were purchased from Sigma (St. Louis, MO). pcDNA3.1-H-RAS N17 [31] was obtained from David Stokoe of ONYX Pharmaceuticals (Richmond, CA).

### 2.2. Cell culture, transfection and reporter analysis

NIH3T3 cells were maintained in DMEM supplemented with 10% FBS and 1 mM penicillin–streptomycin, and EGFR $-/-$  fibroblast, WA-2, and WA-2-FR fibroblasts cells [32] were cultured in RPMI supplemented with 10% FBS and 1 mM penicillin–streptomycin. The NIH3T3 cells were plated onto 6-well plates at 40% confluence. Cell transfections were performed using Lipofectamine plus transfection reagent according to the manufacturer's instructions (Invitrogen, Carlsbad, CA). Forty eight h after transfection, cells were treated with 0.5  $\mu$ g/ml of DKK-1 for 30 min before treating with 150 ng/ml of recombinant WNT3a for an additional 8 h. The cells were then rinsed in ice-cold phosphate buffered saline (PBS) twice and re-suspended in reporter lysis buffer (Promega, Madison, WI) for a Luciferase assay. Luciferase activities were normalized using  $\beta$ -galactosidase levels as an internal control. Transfection efficiencies were normalized by transfection of 50 ng of pCMV  $\beta$ -gal reporter (Clontech, Mountain view, CA).

### 2.3. Western blot analysis

NIH3T3 cells grown in DMEM with 10% FBS were treated with 150 ng/ml of WNT3a or 20 ng/ml of EGF, and then harvested at different times for Western blot analysis [33]. Where required, 200 nM, 20, 40, 60  $\mu$ M of AG1478 or 0.5  $\mu$ g/ml of DKK-1 were applied 30 min before treating with 150 ng/ml of recombinant WNT3a or 20 ng/ml of EGF. For transient transfection analysis, the NIH3T3 cells were transfected with pcDNA3.0 or pcDNA3.1-H-RAS N17. The cells were harvested for Western blot analysis 48 h after transfection. Where required, 150 ng/ml of recombinant WNT3a was applied 30 min before harvesting. For preparation of proteins, attached cells were rinsed twice in ice-cold PBS, harvested, then lysed directly in Laemmli sodium dodecyl sulfate (SDS) sample buffer. Samples were then boiled and subjected to 8–12% SDS-polyacrylamide gel electrophoresis (SDS-PAGE) followed by Western blot analysis using anti-p-ERK, -ERK, -p-MEK, -MEK, -p-RAF-1 (Ser-338), -H-RAS-, -EGFR, - $\beta$ -catenin, or  $\alpha$ -tubulin primary antibody, followed by incubation with an appropriate HRP-conjugated secondary antibody. Protein bands were visualized using an ECL.

### 2.4. Measurement of RAS activation

The capacity of RAS-GTP to bind to the RAS-binding domain of RAF-1 (RBD) was used to analyze the activation status of RAS [34]. Cells were lysed in a culture dish with RAS extraction buffer (20 mM Tris–HCl pH 7.5, 2 mM EDTA, 100 mM NaCl, 5 mM MgCl<sub>2</sub>, 1% Triton X-100, 5 mM NaF, 10% glycerol, 0.5% 2-mercaptoethanol) plus protease inhibitors. Cleared lysate was subjected to a RAS-GTP assay as the manufacturer's instructions (Upstate Biotechnology). The amount of RAS in the bound fraction was determined by Western blot analysis with the anti-Pan-RAS antibody.

### 2.5. siRNA preparation and treatment

Mouse EGFR (Gene bank accession number NM\_207655) mRNA target sequences was designed using a siRNA template design tool (Ambion). The EGFR mRNA target sequences were 5'-AATGGACTTACAGAGCCATCC-3' (531–551) and 5'-AAAGAAGACGCTTCTTGACAG-3' (3181–3201). Each siRNA was synthesized using a *Silencer*<sup>TM</sup> siRNA construction kit (Ambion). The control siRNA was provided from Ambion (Cat#4605). The resulting siRNAs were transfected into NIH3T3 cells at a concentration of 1.68  $\mu$ g per 3.5 cm dish [35]. The transfected cells were grown for 48 h at 37 °C in a 5% CO<sub>2</sub> incubator, then harvested for Western blot analysis.

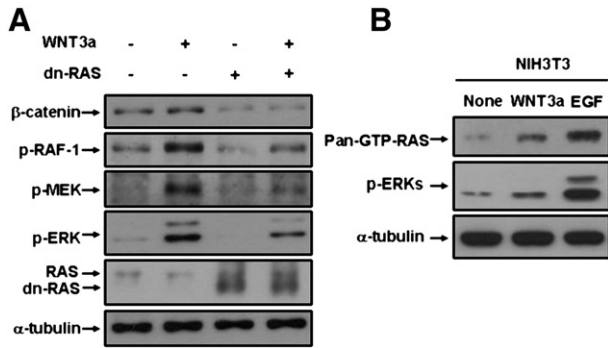


Fig. 1. Effects of WNT3a on activation of RAS-ERK pathway. (A) NIH3T3 cells were grown to 50% confluence in DMEM with 10% FBS, and transfected with either 0.5  $\mu$ g of pcDNA3.0 or pcDNA3.1-H-RAS N17. Forty-eight hours after transfection, 150 ng/ml of recombinant WNT3a was applied for 30 min before harvesting. Whole-cell lysates were subjected to Western blotting using the anti- $\beta$ -catenin-, -p-RAF-1-, -p-MEK-, -p-ERK-, -H-RAS- or - $\alpha$ -tubulin-primary antibody. (B) NIH3T3 cells were grown to 70% confluence and either not treated or treated with 150 ng/ml of recombinant WNT3a or 20 ng/ml of EGF for 30 min. A RAS pull-down analysis was performed to detect GTP-loaded active RAS [34] as described in Materials and methods. Western blot analyses were performed on the whole-cell lysates to detect p-ERK and  $\alpha$ -tubulin. The GTP loaded Pan-RAS protein (RAS-GTP) was also detected by Western blot analysis by using the anti-Pan-RAS antibody.

## 2.6. BrdU incorporation and cytoskeleton staining

Cells were plated onto coverslips as a 40% confluent, then treated with 100 ng/ml of recombinant WNT3a in DMEM supplemented with 1% FBS. Where required, 20  $\mu$ M of AG1478 or 0.25  $\mu$ g/ml of DKK-1 protein were added 30 min before WNT3a treatment. For siRNA treatment, the cells were transfected either with or without 1.68  $\mu$ g of siRNA in a 3.5 cm dish. Twenty-four h after transfection, the cells were treated with 100 ng/ml of recombinant WNT3a in DMEM supplemented with 2% FBS for 24 h before immunocytochemical analysis. For bromodeoxyuridine (BrdU) incorporation measurements, cells were grown for 5 h in DMEM containing 20  $\mu$ M BrdU before immunocytochemical analysis. The cells were washed twice in PBS, fixed in a methanol/formaldehyde (99:1) mixture, and permeabilized with PBS containing 0.2% Triton X-100. The cells were then fixed in 3.7% formaldehyde for 10 min before being incubated for 30 min in 2 N HCl. After being blocked with PBS containing 1% BSA, the cells were incubated with anti-BrdU monoclonal antibody at a dilution of 1:20 for 2 h, then washed with PBS. Alexa Fluor 488 goat anti-mouse IgG secondary antibody, at a dilution of 1:200, was added, and then the cells were incubated for 1 h. In order to stain the nuclei, DAPI was applied at a final concentration of 1  $\mu$ M in PBS for 10 min, and then the cells were washed in distilled water. For cytoskeleton staining, the cells were fixed with 3.7% formaldehyde for 10 min, then permeabilized and blocked, and then incubated with Alexa Fluor 488 phalloidin (1:50) for 30 min. For staining nuclei, DAPI was applied for 10 min, then the cells were mounted. Samples were mounted for photography on a Radiance 2100 Laser Scanning System (Bio-Rad, UK). Each analysis was performed at least three times.

## 2.7. Cell migration assays

For wound-healing assays, cells were grown in DMEM with 10% FBS. After the cells were grown to 70% confluence in the dishes (Corning Inc., NY) that had been pre-coated with fibronectin (10  $\mu$ g/ml, Sigma), they were scratched with a 1 ml pipette tip. Where required, 20  $\mu$ M of AG1478 was added for 30 min before WNT3a (100 ng/ml) treatment for 24 h. A trans-well assay was performed with a 12  $\mu$ m pore size micell cell culture plate insert (Millipore, Bedford, MA) and a 24 well plate (Corning Inc.). For siRNA treatment, the cells were transfected with or without 1.68  $\mu$ g of siRNA in a 3.5 cm dish. After 24 h, the cells were trypsinized, re-suspended with serum-

free DMEM, and plated onto the upper chamber ( $2 \times 10^4$ ). The same volume of serum-free DMEM with or without WNT3a was loaded onto the lower chamber, and incubated for 24 h at 37  $^{\circ}$ C in a 5% CO<sub>2</sub> incubator. Then, the upper chamber and media were removed, and the attached cells in the lower chamber were stained with 0.5% crystal violet. The cells were viewed under 200 $\times$  magnifications using a Nikon Eclipse TE2006-U fluorescence microscope (Model; LHS-H 100P-1).

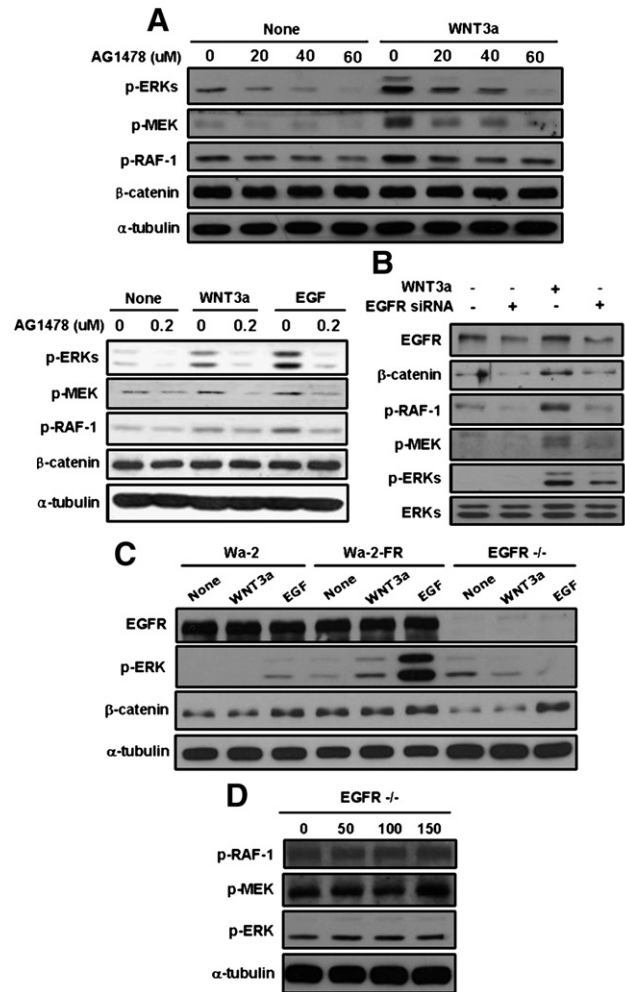


Fig. 2. Effects of AG1478, EGFR siRNA or EGFR defects on WNT3a-induced activation of ERK pathway. (A) NIH3T3 cells were grown to 70% confluence and either not treated or treated with 150 ng/ml of recombinant WNT3a for 30 min. Upper panel: where required, the cells were pre-treated with 0, 20, 40 or 60  $\mu$ M of AG1478 at 30 min before treatment of WNT3a. Lower panel: NIH3T3 cells were grown in DMEM containing 2% FBS for 24 h, and pre-treated with 200 nM of AG1478 at 30 min before treatment of WNT3a or EGF. Western blot analyses were performed using the anti-p-ERK-, p-MEK-, p-RAF-1-,  $\beta$ -catenin- or - $\alpha$ -tubulin-antibody. (B) NIH3T3 cells were either non-transfected or transfected with EGFR siRNA for 48 h. The cells were then treated with 150 ng/ml of recombinant WNT3a for 30 min before harvesting. Western blot analyses were performed to detect EGFR,  $\beta$ -catenin, p-RAF-1, p-MEK, p-ERK or ERK. (C) Wa-2, Wa-2-FR, and EGFR<sup>-/-</sup> knock-out fibroblasts (Materials and methods) were grown to 70% confluence and treated with 150 ng/ml of recombinant WNT3a or 20 ng/ml of EGF for 30 min. The cells were harvested, and Western blot analyses were performed to detect EGFR, p-ERK,  $\beta$ -catenin or  $\alpha$ -tubulin. (D) EGFR<sup>-/-</sup> knock-out fibroblasts were grown to 70% confluence and treated with different concentrations of recombinant WNT3a (0, 50, 100, and 150 ng/ml) for 30 min. The cells were harvested, and Western blot analyses were performed to detect p-RAF-1, p-MEK, p-ERK, or  $\alpha$ -tubulin.

### 3. Results

#### 3.1. WNT3a immediately activates the RAS-RAF-1–MEK–ERK kinase module

The RAF-1, MEK and ERK kinases were concomitantly activated by 30 min treatment of WNT3a in NIH3T3 cells (Fig. 1A) [19]. The total  $\beta$ -catenin level, however, was not significantly affected by 30 min treatment of WNT3a (Figs. 1A and 2A) [19]. However,  $\beta$ -catenin was translocated at the membrane of the NIH3T3 cells by 30 min treatment of WNT3a [19]. To identify involvement of the upstream component RAS in the WNT3a-induced activation of the ERK pathway, we measured the effect of dominant-negative RAS (dn-RAS) in the WNT3a-induced ERK activation. The ERK activity increased by WNT3a was also reduced by transfection of dn-RAS (Fig. 1A). Involvement of RAS in WNT3a-induced ERK activation was further confirmed by the increase of the level of GTP-RAS in the WNT3a-treated NIH3T3 cells (Fig. 1B).

#### 3.2. WNT3a activates the ERK pathway through EGFR

Immediate activation of the ERK pathway by WNT3a occurred independently of  $\beta$ -catenin [19], and WNT3a acted on the ERK pathway independently of Fzd [20]. These results indicate the involvement of upstream components of the ERK pathway, such as EGFR, in WNT3a-induced ERK pathway activation. To identify the involvement of EGFR in WNT3a-induced ERK pathway activation, NIH3T3 cells were pre-treated dose-dependently with AG1478, the EGFR inhibitor, and the effect on WNT3a in the ERK pathway activation was measured. The WNT3a-induced activations of RAF-1, MEK, and ERK kinases were inhibited by AG1478 in dose-dependent manner (Fig. 2A; upper panel). The basal activities of the RAF-1, MEK, and ERK kinases were also inhibited by AG1478 in a dose-dependent manner (Fig. 2A; upper panel). The basal activities and EGF-/WNT3a-induced activations of the ERK pathway components were also inhibited by a lower concentration of AG1478 (200 nM) (Fig. 2A; lower panel).

To further confirm the role of EGFR in WNT3a-induced ERK pathway activation, we measured the effects of EGFR siRNA on WNT3a-induced ERK pathway activation. The WNT3a-induced RAF-1, MEK, and ERK kinase activations were inhibited by EGFR siRNA (Fig. 2B). The basal ERK pathway activations were also inhibited by EGFR siRNA (Fig. 2B). Interestingly, the level of total  $\beta$ -catenin was also reduced by EGFR siRNA (Fig. 2B). The role of EGFR in WNT3a-

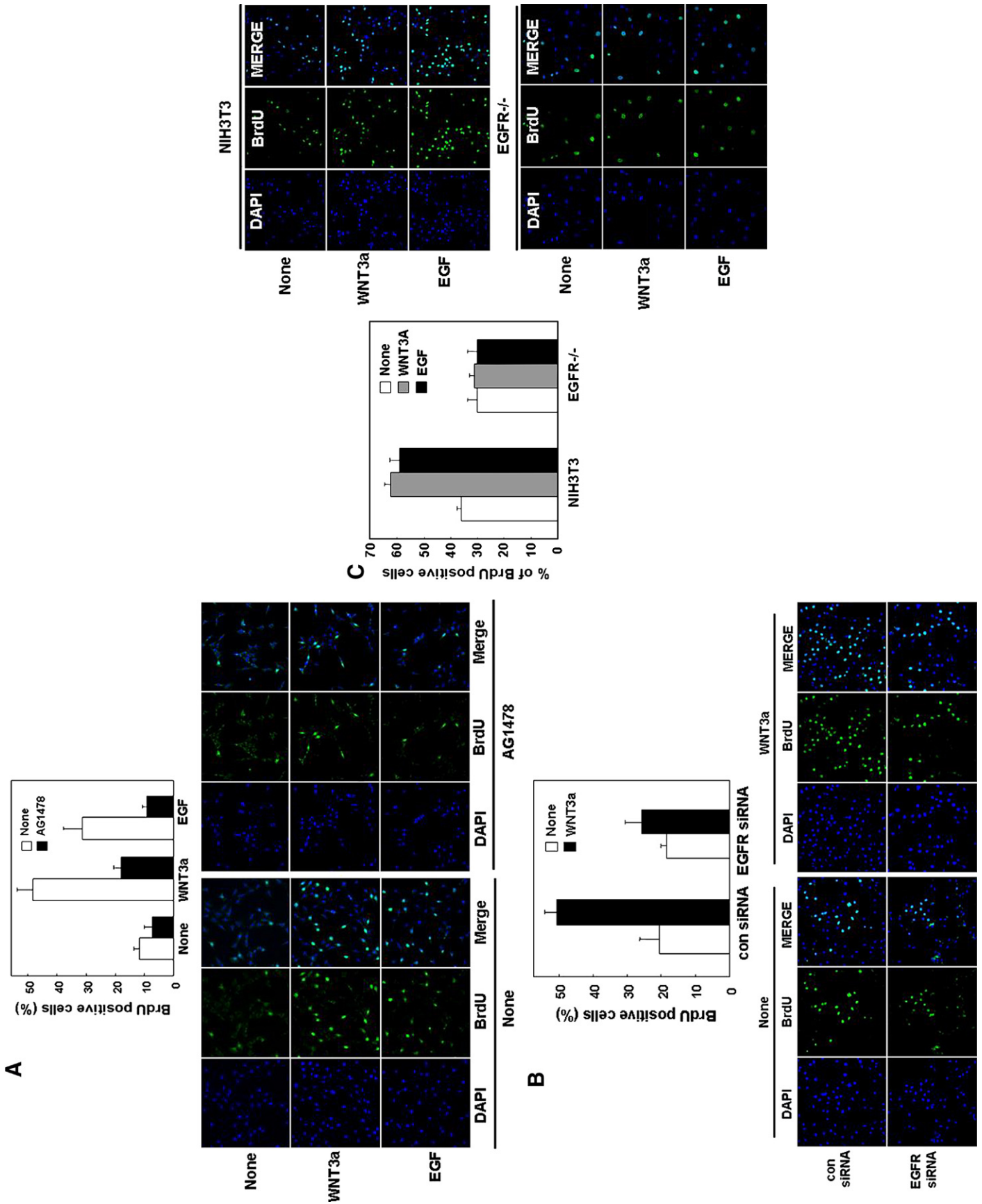
induced activation of the ERK pathway was further confirmed in fibroblasts that either lack expression of EGFR (EGFR<sup>-/-</sup>) or express an autophosphorylation-defective EGFR mutant, Wave-2 (Wa-2) [32]. ERK activity was weakly increased by EGF treatment but not increased by WNT3a in the Wa-2 fibroblast (Fig. 2C). WNT3a-induced ERK activation was restored in Wa-2 cells reconstituted with the wild-type EGFR, Wa-2-EGFR (Fig. 2C). However, the level of ERK activation by WNT3a was less significant than that by EGF (Fig. 2C). The level of total  $\beta$ -catenin was also higher in Wa-2-EGFR fibroblasts than in Wa-2 fibroblasts (Fig. 2C). The total  $\beta$ -catenin level was lowest in EGFR<sup>-/-</sup> fibroblasts (Fig. 2C). The ERK activations by WNT3a and EGF were totally abolished in the EGFR<sup>-/-</sup> fibroblasts (Fig. 2C). Interestingly, the level of  $\beta$ -catenin was increased by EGF stimulation in Wa-2 and EGFR<sup>-/-</sup> fibroblasts, and the levels are similar to that of Wa-2-FR (Fig. 2C). The ERK activities did not increase, even after treatment with WNT3a at concentration as high as 150 ng/ml in EGFR<sup>-/-</sup> fibroblasts (Fig. 2D).

#### 3.3. EGFR is involved in WNT3a-induced proliferation of cells

To identify the involvement of EGFR in WNT3a-induced cell proliferation, we measured the effect of AG1478 on the cell proliferation by WNT3a. The percentage of BrdU incorporating cells was increased approximately 4-fold (from 12% to 48%) by WNT3a, 3-fold (from 12% to 33%) by EGF (Fig. 3A; lower panels show representative data). The percentage of BrdU incorporating cells was reduced from 11.6% to 7% by AG1478 at the basal status. The WNT3a-induced cell proliferation was more significantly reduced (from 48% to 18%) by AG1478, and likewise, the percentage of BrdU positive cells was reduced (from 33% to 8.9%) by AG1478 in EGF-treated cells (Fig. 3A; lower panels show representative data).

The role of EGFR in WNT3a-induced proliferation was further confirmed by measurement of the effect of EGFR siRNA (Fig. 3B). The percentage of BrdU positive cells was increased by WNT3a (20% to 50%), whereas WNT3a-induced cell proliferation was significantly reduced (50% to 25%) by treatment of EGFR siRNA (Fig. 3B; lower panels show representative data). To further confirm the role of EGFR in WNT3a-induced cell proliferation, we used EGFR<sup>-/-</sup> fibroblast cells and NIH3T3 cells as a control for a BrdU incorporation assay. In the NIH3T3 cells, the percentage of BrdU positive cells was increased by WNT3a (36% to 63%) and EGF (36% to 59%) (Fig. 3C; right panels show representative data). The EGFR<sup>-/-</sup> fibroblast cells, however, did not affect proliferation by treatment of either WNT3a or EGF (Fig. 3C).

Fig. 3. Effects of AG1478, EGFR siRNA or EGFR knock-out on WNT3a-induced proliferation of NIH3T3 fibroblast. (A) NIH3T3 cells were grown on coverslips in DMEM and either non-treated or treated with 100 ng/ml of recombinant WNT3a or 20 ng/ml of EGF for 24 h. Where required, the cells were pre-treated with 20  $\mu$ M of AG1478 for 30 min before treatment of WNT3a. (B) NIH3T3 cells were grown on cover slides in DMEM and either non-transfected or transfected with 1.68  $\mu$ g of EGFR siRNA per 3.5 cm dish for 48 h. Where required, 100 ng/ml of recombinant WNT3a was applied for 24 h before fixing. (C) NIH3T3 and EGFR<sup>-/-</sup> fibroblast cells were grown as described above. Where required, 100 ng/ml of recombinant WNT3a or 20 ng/ml of EGF was applied for 24 h before fixing. The cells were labeled with 20  $\mu$ M BrdU for 5 h prior to immunocytochemical analysis. The cell nuclei were stained with DAPI. The cells containing BrdU incorporated into the nucleus were scored as BrdU positive cells. Upper or left panel: results of a quantitative measurement of percentage of BrdU positive cells. Analyses were performed at least three times and 100 cells were counted in each case. The error bars represent the standard deviations of three independent analyses. The representative data for each quantitative result are provided.



### 3.4. EGFR is involved in WNT3a-induced cell motility

Cell motility and invasion are important cellular processes in the proliferation and transformation of cells [36,37]. WNTs are

involved in the motility and invasion of cells involved in cytoskeletal rearrangement [23,24,26]. EGFR is also known as a regulator of cell motility and invasion related to cytoskeletal rearrangement [27,38]. However, the interrelationship between

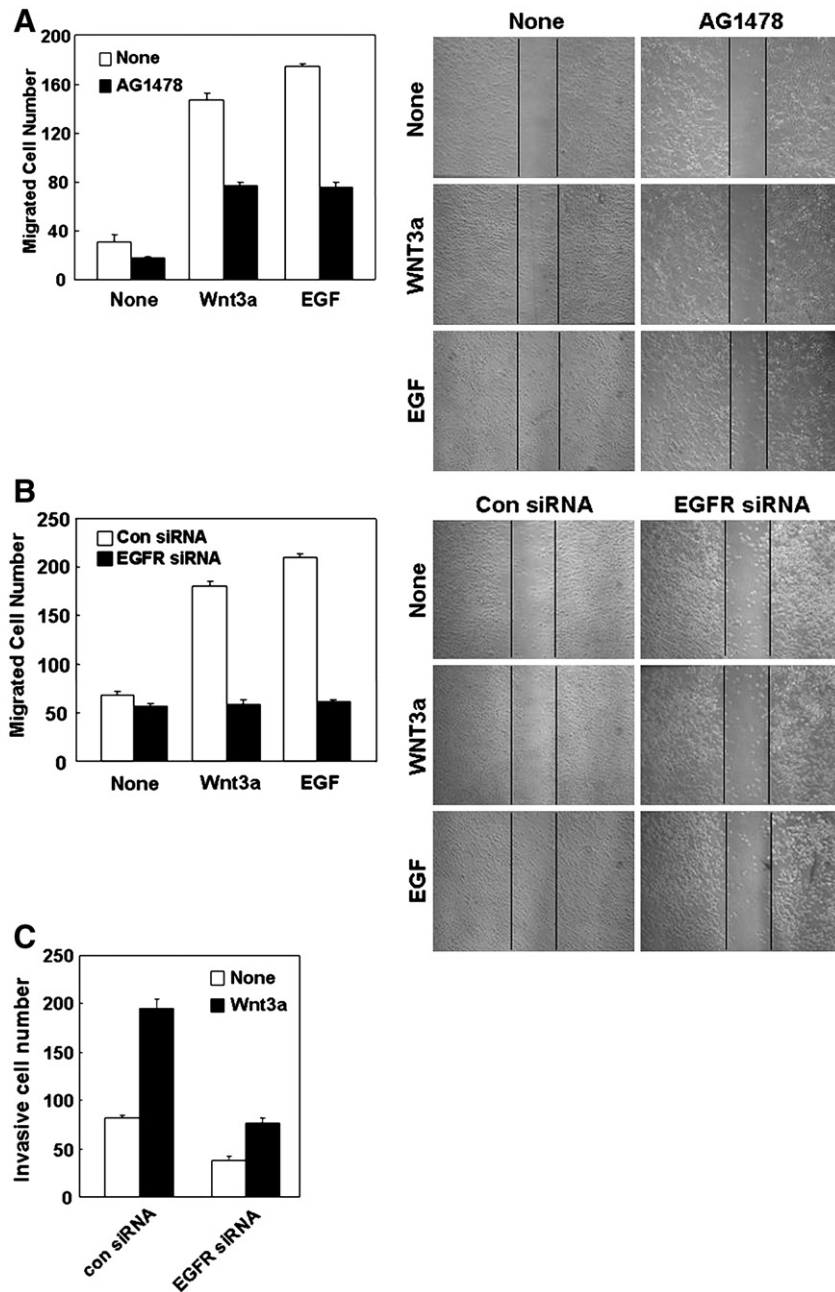


Fig. 4. Effects of AG1478 or EGFR siRNA on WNT3a-induced cell motility. (A) NIH3T3 cells were grown in DMEM on fibronectin-coated dishes and scratched with a pipette. The cells were non-treated or treated with 100 ng/ml of recombinant WNT3a or 20 ng/ml of EGF for 24 h. Where required, 20  $\mu$ M of AG1478 was pre-treated for 30 min before treatment of WNT3a or EGF. The graph represents the quantitative results for the number of cells migrating to the defined unit area. Analyses were performed at least three times, and the error bars indicate the standard deviations of three independent analyses. Representative data for the results are shown in the right panels. (B) NIH3T3 cells were grown in DMEM on fibronectin-coated dishes, and either non-transfected or transfected with 1.68  $\mu$ g of EGFR siRNA per 3.5 cm dish for 24 h. Before being scratched with a pipette, the cells were non-treated or treated with 100 ng/ml of recombinant WNT3a or 20 ng/ml of EGF for 24 h. The graph represents the quantitative results for the number of cells migrating to the defined unit area. Analyses were performed at least three times and the error bars indicate the standard deviations of three independent analyses. Representative data for the results are shown in the right panels. (C) NIH3T3 cells were grown in DMEM, and either non-transfected or transfected with 1.68  $\mu$ g of EGFR siRNA per 3.5 cm dish for 24 h. The cells were trypsinized and plated onto the upper chamber, and serum-free DMEM with 100 ng/ml of recombinant WNT3a was applied in the lower chamber. The migrated cells that were transferred from the upper chamber to the lower chamber were stained with 0.5% crystal violet for counting purpose. The experiments were performed at least three times. The error bars are standard deviations of three independent analyses.

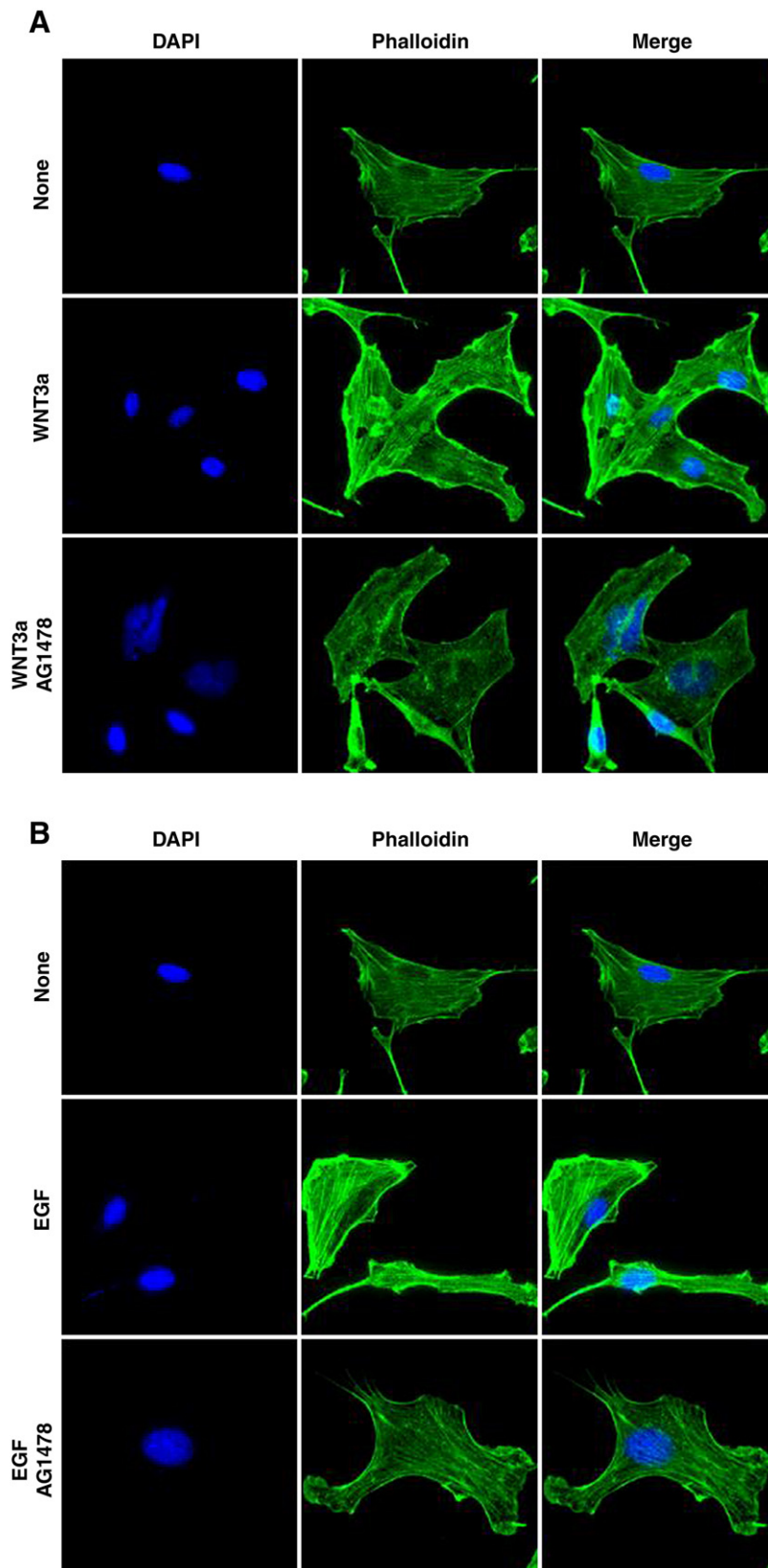


Fig. 5. Effects of AG1478 on WNT3a-induced cytoskeletal rearrangement. (A) NIH3T3 cells were grown in DMEM on coverslips. The cells were treated with 100 ng/ml of recombinant WNT3a or (B) 20 ng/ml of EGF for 30 min. Where required, 20  $\mu$ M of AG1478 was applied for 30 min before treatment of WNT3a or EGF. The cells were fixed and stained with Alexa Fluor 488 phalloidin for observation with the Radiance 2100 Laser Scanning System (Bio-Rad). The cell nuclei were stained with DAPI.

WNTs and EGFR in the regulation of cell motility and cytoskeletal rearrangement is not characterized. To identify the role of EGFR in WNT3a-induced cell motility, we performed an *in vitro* wound-healing assay using AG1478 and EGFR siRNA. The number of migrated cells was increased by 24 h after WNT3a treatment (Fig. 4A and B; qualitative data are shown in right panels). The WNT3a-induced cell migration was reduced to almost basal levels by AG1478 and EGFR siRNA (Fig. 4A and B). The EGF-induced cell migration, although the level of increase was relatively low, was also reduced by AG1478 and EGFR siRNA (Fig. 4A and B). To further confirm the role of EGFR in WNT3a-induced cell

migration, we performed a trans-well invasion assay. The invasive cell numbers were increased by 24 h WNT3a treatment (Fig. 4C), and the WNT3a-induced cell invasion was also reduced by EGFR siRNA (Fig. 4C).

The cytoskeletal rearrangement is directly related to the movement and invasion of cells [39,40]. To confirm the role of EGFR in WNT3a-induced cytoskeletal rearrangement, we measured the pattern of phalloidin staining. WNT3a induced the cytoskeletal rearrangement and the formation of the stress fiber and the lamellipodia, an essential structure in cell movement and invasion within 30 min [41,42] (Fig. 5A). WNT3a-induced cytoskeletal rearrangement and stress fiber

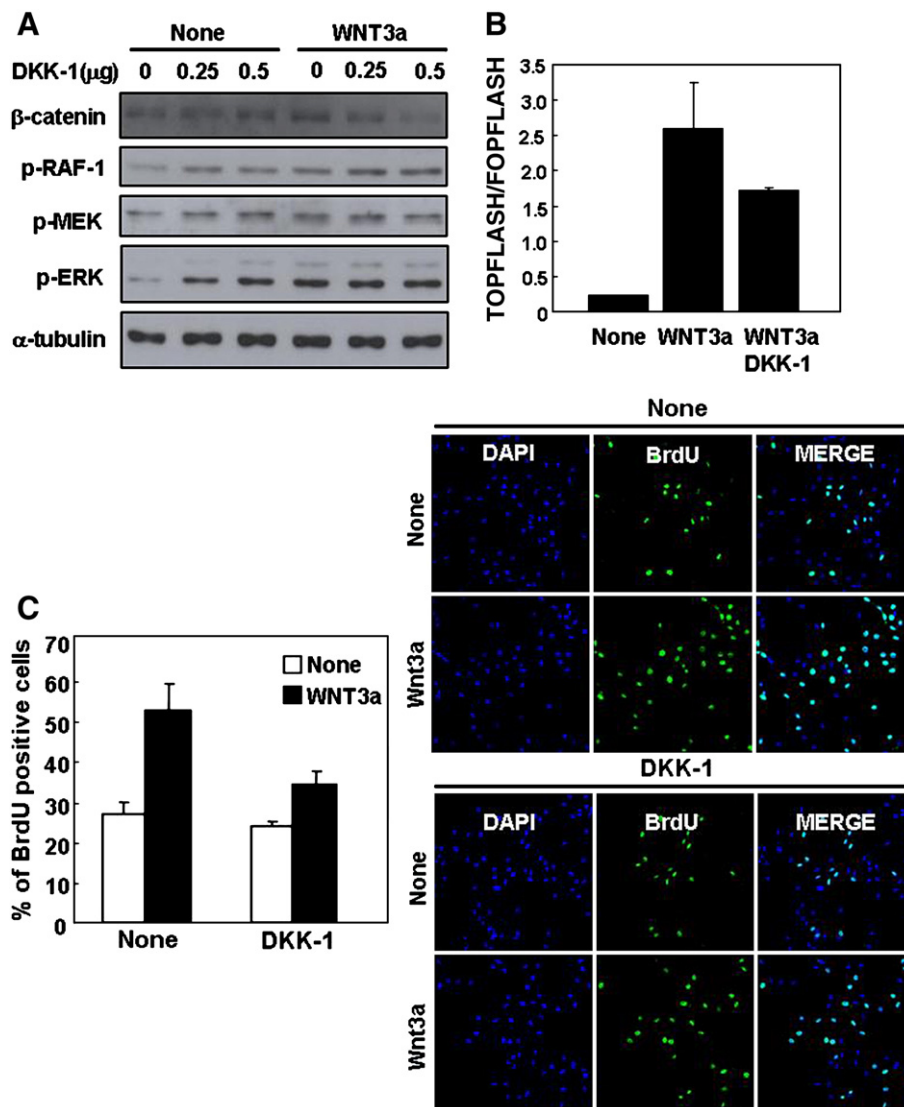


Fig. 6. Effects of Dickkopf-1 on WNT3a-induced ERK pathway activation and proliferation of NIH3T3 cells. (A) NIH3T3 cells were grown in DMEM, and either non-treated or treated with 150 ng/ml of recombinant WNT3a for 30 min before harvesting. Where required, cells were pre-treated with 0, 0.25 or 0.5  $\mu$ g/ml of recombinant DKK-1 for 30 min before treatment of WNT3a. Western blot analyses were performed as described in Fig. 2. (B) NIH3T3 cells were grown to 50% confluence, then transfected with either 0.5  $\mu$ g of pTOPFLASH or pFOPFLASH [43]. Forty-eight hours after transfection, cells were treated with 150 ng/ml of recombinant WNT3a for 8 h before harvesting for a luciferase assay. Where required, 0.5  $\mu$ g/ml of recombinant DKK-1 was applied 30 min before WNT3a treatment. The mean values and standard deviations of three independent experiments are shown. (C) NIH3T3 cells were grown in DMEM on coverslips and either non-treated or treated with 100 ng/ml of recombinant WNT3a for 24 h. Where required, cells were pre-treated with 0.25  $\mu$ g/ml of DKK-1 for 30 min before treatment of WNT3a. The cells were labeled with 20  $\mu$ M BrdU for 5 h prior to immunocytochemical analysis. The cell nuclei were stained with DAPI. The images were obtained with the Radiance 2100 Laser Scanning System. The cells incorporated BrdU in their nucleus were scored as BrdU positive cells. Analyses were performed at least three times, and the error bars indicate the standard deviations of three independent analyses. Representative data for the results are shown in the right panels.



and lamellipodia formation were reduced by co-treatment of AG1478 (Fig. 5A). EGF-induced cytoskeletal rearrangement and lamellipodia formation were also blocked by co-treatment of AG1478 (Fig. 5B).

### 3.5. WNT3a-induced immediate ERK activation occurs independently of WNT/ $\beta$ -catenin pathway

To identify the involvement of WNT/ $\beta$ -catenin in WNT3a-induced ERK pathway activation, we measured the effects of DKK-1, the inhibitor of the Fzd co-receptor, LRP5/6, in WNT3a-induced ERK activation. The WNT3a-induced activations of RAF-1, MEK, and ERK kinases were not inhibited by pre-treatment of DKK-1 (Fig. 6A). The total  $\beta$ -catenin level was, however, reduced in a dose-dependent manner, indicating the normal functionality of DKK-1 in the inhibition of WNT3a-induced activation of the WNT/ $\beta$ -catenin pathway. The basal levels of RAF-1, MEK, and ERK kinase activities were up-regulated by DKK-1 in a dose-dependent manner (Fig. 6A) by an unknown mechanism. The transcriptional reporter activity of the WNT/ $\beta$ -catenin pathway measured according to the ratio of the luciferase activity from pTOPFLASH and pFOPFLASH [43] was also increased, approximately 9-fold, by WNT3a treatment (Fig. 6B). The WNT3a-induced activation of pTOPFLASH/pFOPFLASH reporter activity was also down-regulated with  $\beta$ -catenin reduction by DKK-1 [30,44] (Fig. 6B). To identify the role of WNT/ $\beta$ -catenin pathway in WNT3a-induced cell proliferation, we measured the effects of DKK-1 on WNT3a-induced BrdU incorporation. The WNT3a-induced BrdU incorporation was down-regulated by DKK-1 protein (53% vs 35%) (Fig. 6C; right panels show representative qualitative data).

## 4. Discussion

The WNT signaling pathways are involved in the regulation of differentiation, organogenesis, adipogenesis, proliferation, and motility [6,45–47]. The WNT pathways are activated by various WNT proteins, including WNT1, WNT2, WNT2b, WNT3a, WNT5b, WNT7b, and WNT8a, and others [48,49], several of which induce cell growth and transformation [46,50,51]. WNT signals transduce through at least three distinct intracellular pathways; the WNT/ $\beta$ -catenin signaling pathway (often called the canonical WNT pathway), the WNT/ $\text{Ca}^{2+}$  pathway, and the WNT/polarity pathway (reviewed in [49,52,53]). The WNT/ $\beta$ -catenin pathway is activated by WNT1, WNT3, WNT3a, WNT7a, and WNT8, and is involved in cellular proliferation, transformation, and motility [49,54]. WNT3a activates cell motility through cytoskeleton rearrangement in myeloma plasma cells [26], and ovary cells [23]. The WNT3a induced motility of cells attributed by activation of RhoA [23], but involvement of the ERK pathway in that process is not known. WNT3a activates the proliferation of chick somites [54], human mesenchymal stem cells [55] and multiple myeloma cells [56]. It stimulates the proliferation of mouse fibroblasts, at least partly via activation of the ERK pathway [19]. However, the route for activation of the ERK pathway,

especially at upstream level, was only poorly characterized. Treatment of WNT3a immediately increased the activities of the RAF-1, MEK and ERK kinases, and the effects of WNT3a were reduced by transfection of dn-RAS. The involvement of RAS in the WNT3a-induced ERK pathway activation was further evidenced by the increase of the level of GTP-bound RAS (GTP-RAS) by WNT3a treatment. The WNT3a-induced activation of the ERK pathway was abolished by the EGFR inhibitor, AG1478, indicates the role of EGFR in WNT3a-induced ERK pathway activation, and that was supported by genetic approaches using EGFR siRNA (Fig. 2B). The role of EGFR in the WNT3a-induced ERK pathway activation was further confirmed by measuring the effect of WNT3a in both fibroblasts retaining knocked-out and functionally defective EGFR (Fig. 2C and D), which did not show the effects of WNT3a in the ERK activation. The role of EGFR in WNT3a-induced ERK pathway activation, however, might be partial, which indicates the possibility of the involvement of other receptor(s) such as platelet derived growth factor receptor and Frizzled receptor etc. To identify the involvement of the WNT/ $\beta$ -catenin pathway in the immediate ERK activation by WNT3a, we investigated the effect of DKK-1 on the ERK activation by WNT3a. The ERK pathway activation by WNT3a was not affected, although the total  $\beta$ -catenin level and WNT/ $\beta$ -catenin reporter activity were reduced by DKK-1 (Fig. 6A and B). These results indicate that the classical WNT/ $\beta$ -catenin pathway is not involved in immediate ERK activation by WNT3a. The ERK pathway components were dose-dependently increased by DKK-1 in cells non-treated with WNT3a (Fig. 6A). Currently, the mechanism of basal ERK pathway activation by DKK-1 is not understood. Those results, however, indicate that DKK-1 activates the ERK pathway independently of WNT3a. Except the immediate activation, ERK activation can also occur in a prolonged manner by WNT3a treatment, and is related to Tcf-4/ $\beta$ -catenin-mediated transcriptional activation [19]. Long term ERK pathway activation via  $\beta$ -catenin/Tcf mediated transcription can occur via induction of EGFR, one of the transcriptional target genes of the  $\beta$ -catenin/Tcf transactivator [57].

The ERK pathway is involved in WNT3a-induced cell proliferation and growth [19]. WNT3a-induced growth stimulation was significantly reduced by AG1478, indicating the involvement of EGFR in WNT3a-induced proliferation. The role of EGFR in WNT3a-induced cell proliferation was further confirmed by experiments using EGFR siRNA and defective EGFR cell lines. WNT3a-induced cellular proliferation was also decreased by DKK-1 treatment which reduced the total  $\beta$ -catenin level without inhibiting the RAF-1, MEK and ERK activities (Fig. 6C). These results indicate that the reduction of WNT3a-induced proliferation by DKK-1 might occur independently of immediate activation of the ERK pathway components. The extent of the reduction of WNT3a-induced proliferation by DKK-1 (52% to 35%) was lower than that by ERFR inhibitor (48% to 18%) or EGFR siRNA (50% to 25%) (compare Figs. 3A, B, and 6C). The low fold reduction of WNT3a-induced proliferation by DKK-1 might be due to the fact that DKK-1 may inhibit WNT3a-induced proliferation only

via the WNT/ $\beta$ -catenin pathway involving Tcf-4/ $\beta$ -catenin-mediated post gene transcription [19]. The extent of inhibition of the WNT3a-induced proliferation by the AG1478 or EGFR siRNA was higher than that by DKK-1, and that might reflect the fact that both of the WNT3a-induced proliferating signals mediated by EGFR, via the WNT/ $\beta$ -catenin pathway and immediate signaling activation of ERK pathway, are blocked by the EGFR inhibitors. The WNT3a-induced proliferation can also be acquired by activation of the WNT/ $\beta$ -catenin pathway via EGFR as shown by decrease of  $\beta$ -catenin in Wa-2 and EGFR $^{-/-}$  fibroblasts and EGFR siRNA treated cells (Fig. 2B and C). Therefore, reduction of WNT3a-induced proliferation by EGFR inhibitors can also be attributed by inhibition of the WNT/ $\beta$ -catenin pathway via EGFR. Overall, proliferation by WNT3a is attributed to both the WNT/ $\beta$ -catenin and ERK pathways. In addition, the WNT/ $\beta$ -catenin or ERK pathway transmit proliferation signals by tight cross-talk at various levels including Tcf/ $\beta$ -catenin mediated transcriptions and immediate EGFR signaling which involves activation of both the WNT/ $\beta$ -catenin and ERK pathways.

WNT3a is involved in cell motility and cytoskeletal rearrangement, and RhoA and DSH are known mediators of this process [23,26]. WNT3a-induced migration and invasion of cells were inhibited by AG1478 and EGFR siRNA (Fig. 4A and B), indicating that EGFR is also involved in WNT3a-induced cell motility. The role of EGFR in WNT3a-induced motility was further confirmed by the inhibition of the cytoskeletal rearrangement including lamellipodia formation, by AG1478. These results further indicate that EGFR is involved in WNT3a-induced cytoskeletal regulation leading to cell movement and invasion.

In this study, we identified the role of EGFR in the WNT3a-induced immediate activation of the ERK pathway involving motility and proliferation of fibroblasts. The WNT3a induced proliferation via EGFR is attributed to both the WNT/ $\beta$ -catenin and ERK pathways involving complex cross-talk.

## Acknowledgments

The authors thank Drs. Tony Burgers and Francesca Walker for providing Wa-2, Wa-2-FR, and EGFR $^{-/-}$  cell lines. This work was supported by the Korea Science and Engineering Foundation (KOSEF) grant funded by the Korea government (MOST) (No. 2005–01564; 2006–02681; R112000078010020). S.E. Kim was supported by a BK21 studentship from the ministry of education and human resources development.

## References

- [1] K. Willert, J.D. Brown, E. Danenberg, A.W. Duncan, I.L. Weissman, T. Reya, J.R. Yates, R. Nusse, *Nature* 423 (2003) 448.
- [2] R.T. Moon, B. Bowerman, M. Boutros, N. Perrimon, *Science* 296 (2002) 1644.
- [3] R. Widelitz, *Growth Factors* 23 (2005) 111.
- [4] A. Kikuchi, S. Kishida, H. Yamamoto, *Exp. Mol. Med.* 38 (2006) 1.
- [5] J.D. Brown, R.T. Moon, *Curr. Opin. Cell Biol.* 10 (1998) 182.
- [6] T. Akiyama, *Cytokine Growth Factor Rev.* 11 (2000) 273.
- [7] S. Ikeda, S. Kishida, H. Yamamoto, H. Murai, S. Koyama, A. Kikuchi, *EMBO J.* 17 (1998) 1371.
- [8] C. Sakanaka, J.B. Weiss, L.T. Williams, *Proc. Natl. Acad. Sci. U. S. A.* 95 (1998) 3020.
- [9] D.C. Slusarski, V.G. Corces, R.T. Moon, *Nature* 390 (1997) 410.
- [10] H.C. Huang, P.S. Klein, *Genome Biol.* 5 (2004) 234.
- [11] F. Cong, L. Schweizer, H. Varmus, *Development* 131 (2004) 5103.
- [12] T.C. He, A.B. Sparks, C. Rago, H. Hermeking, L. Zawel, L.T. da Costa, P.J. Morin, B. Vogelstein, K.W. Kinzler, *Science* 281 (1998) 1509.
- [13] O. Tetsu, F. McCormick, *Nature* 398 (1999) 422.
- [14] J. Blenis, *Proc. Natl. Acad. Sci. U. S. A.* 90 (1993) 5889.
- [15] J.S. Sebolt-Leopold, *Oncogene* 19 (2000) 6594.
- [16] P. Shapiro, *Crit. Rev. Clin. Lab. Sci.* 39 (2002) 285.
- [17] S. Grant, L. Qiao, P. Dent, *Front. Biosci.* 7 (2002) d376.
- [18] C. Liebmann, *Cell Signal* 13 (2001) 777.
- [19] M.S. Yun, S.E. Kim, S.H. Jeon, J.S. Lee, K.Y. Choi, *J. Cell Sci.* 118 (2005) 313.
- [20] M. Almeida, L. Han, T. Bellido, S.C. Manolagas, S. Kousteni, *J. Biol. Chem.* 280 (2005) 41342.
- [21] G. Civenni, T. Holbro, N.E. Hynes, *EMBO Rep.* 4 (2003) 166.
- [22] I. Oishi, H. Suzuki, N. Onishi, R. Takada, S. Kani, B. Ohkawara, I. Koshida, K. Suzuki, G. Yamada, G.C. Schwabe, S. Mundlos, H. Shibuya, S. Takada, Y. Minami, *Genes Cells* 8 (2003) 645.
- [23] Y. Endo, V. Wolf, K. Muraiso, K. Kamijo, L. Soon, A. Uren, M. Barshishat-Kupper, J.S. Rubin, *J. Biol. Chem.* 280 (2005) 777.
- [24] J. Lyu, C.K. Joo, *J. Biol. Chem.* 280 (2005) 21653.
- [25] L. Ouko, T.R. Ziegler, L.H. Gu, L.M. Eisenberg, V.W. Yang, *J. Biol. Chem.* 279 (2004) 26707.
- [26] Y.W. Qiang, K. Walsh, L. Yao, N. Kedee, P.M. Blumberg, J.S. Rubin, J. Shaughnessy Jr., S. Rudikoff, *Blood* 106 (2005) 1786.
- [27] N. Marcoux, K. Vuori, *Cell Signal.* 17 (2005) 1449.
- [28] Q. Jiang, C. Zhou, Z. Bi, Y. Wan, *J. Ocular Pharmacol. Ther.* 22 (2006) 99.
- [29] B. Mao, W. Wu, Y. Li, D. Hoppe, P. Stanek, A. Glinka, C. Niehrs, *Nature* 411 (2001) 255.
- [30] A. Bafico, G. Liu, A. Yaniv, A. Gazit, S.A. Aaronson, *Nat. Cell Biol.* 3 (2001) 683.
- [31] H. Cai, J. Szeberenyi, G.M. Cooper, *Mol. Cell. Biol.* 10 (1990) 5314.
- [32] K.J. Fowler, F. Walker, W. Alexander, M.L. Hibbs, E.C. Nice, R.M. Bohmer, G.B. Mann, C. Thumwood, R. Maglittio, J.A. Danks, R. Chetty, A.W. Burgess, A.R. Dunn, *Proc. Natl. Acad. Sci. U. S. A.* 92 (1995) 1465.
- [33] S.Y. Oh, K.S. Park, J.A. Kim, K.Y. Choi, *Exp. Mol. Med.* 34 (2002) 27.
- [34] J. De-Rooij, J.L. Bos, *Oncogene* 14 (1997) 623.
- [35] S.M. Elbashir, J. Harborth, W. Lendeckel, A. Yalcin, K. Weber, T. Tuschl, *Nature* 411 (2001) 494.
- [36] R.K. Assoian, X. Zhu, *Curr. Opin. Cell Biol.* 9 (2000) 93.
- [37] J.L. Walker, A.K. Fournier, R.K. Assoian, *Cytokine Growth Factor Rev.* 16 (2005) 395.
- [38] Z. Yang, R. Bagheri-Yarmand, R.A. Wang, L. Adam, V.V. Papadimitrakopoulou, G.L. Clayman, A. El-Naggar, R. Lotan, C.J. Barnes, W.K. Hong, R. Kumar, *Clin. Cancer Res.* 10 (2004) 658.
- [39] S. Li, J.L. Guan, S. Chien, *Annu. Rev. Biomed. Eng.* 7 (2005) 105.
- [40] D. Yamazaki, S. Kurisu, T. Takenawa, *Cancer Sci.* 96 (2005) 379.
- [41] J.V. Small, T. Stradal, E. Vignal, K. Rottner, *Trends Cell Biol.* 12 (2002) 112.
- [42] B. Wehrle-Haller, B. Imhof, *Trends Cell Biol.* 12 (2002) 382.
- [43] V. Korinek, N. Barker, P.J. Morin, D. van Wichen, R. de Weger, K.W. Kinzler, B. Vogelstein, H. Clevers, *Science* 275 (1997) 1784.
- [44] M.V. Semenov, K. Tamai, B.K. Brott, M. Kuhl, S. Sokol, X. He, *Curr. Biol.* 11 (2001) 951.
- [45] W.J. Nelson, R. Nusse, *Science* 303 (2004) 1483.
- [46] P. Polakis, *Genes Dev.* 14 (2000) 1837.
- [47] S.E. Ross, N. Hemati, K.A. Longo, C. Bennett, P.C. Lucas, R.L. Erickson, O.A. MacDougald, *Science* 289 (2000) 950.
- [48] A. Dimitriadis, E. Vincan, I.M. Mohammed, N. Roczo, W.A. Phillips, S. Baidur-Hudson, *Cancer Lett.* 166 (2001) 185.
- [49] J.R. Miller, *Genome Biol.* 3 (2002) 3001.1.
- [50] H. Shimizu, M.A. Julius, M. Giarre, Z. Zheng, A.M. Brown, J. Kitajewski, *Cell Growth Differ.* 8 (1997) 1349.

- [51] G.T. Wong, B.J. Gavin, A.P. McMahon, *Mol. Cell. Biol.* 14 (1994) 6278.
- [52] J. Huelsken, J. Behrens, *J. Cell Sci.* 115 (2002) 3977.
- [53] F.T. Kolligs, G. Bommer, B. Goke, *Digestion* 66 (2002) 131.
- [54] L.M. Galli, K. Willert, R. Nusse, Z. Yablonka-Reuveni, T. Nohno, W. Denetclaw, L.W. Burrus, *Dev. Biol.* 269 (2004) 489.
- [55] D. Boer, H.J. Wang, C. Blitterswijk, *Tissue Eng.* 10 (2004) 393.
- [56] P.W. Derksen, E. Tjin, H.P. Meijer, M.D. Klok, H.D. MacGillavry, M.H. van Oers, H.M. Lokhorst, A.C. Bloem, H. Clevers, R. Nusse, R. van der Neut, M. Spaargaren, S.T. Pals, *Proc. Natl. Acad. Sci. U. S. A.* 101 (2004) 6122.
- [57] X. Tan, U. Apte, A. Micsenyi, E. Kotsagrelis, J.H. Luo, S. Ranganathan, D.K. Monga, A. Bell, G.K. Michalopoulos, S.P. Monga, *Gastroenterology* 129 (2005) 285.